Eur. Phys. J. B **5**, 61–66 (1998)

THE EUROPEAN PHYSICAL JOURNAL B

Magnetic and transport properties of sputtered Fe/Si multilayers

L.N. Tong[1], M.H. Pan[1], J. Wu[1], X.S. Wu[1], J. Du[1], M. Lu[1], D. Feng[1], H.R. Zhai[1,a] and H. Xia[2]

[1] Center of Materials Analysis and National Laboratory of Solid State Microstructures, Nanjing University, CASTM, Nanjing 210093, P.R. China
[2] General Research Institute for Nonferrous Metals, Beijing, 100088, P.R. China

Received: 11 February 1998 / Revised: 9 March 1998 / Accepted: 9 March 1998

Abstract. The structural, magnetic and transport properties of sputtered Fe/Si multilayers were studied. The analyses of the data of the X-ray diffraction, resistance and magnetic measurements show that heavy atomic interdiffusion between Fe and Si occurs, resulting in multilayers of different complicated structures according to different sublayer thicknesses. The nominal Fe layers in the multilayers generally consist of Fe layers doped with Si, ferromagnetic Fe-Si silicide layers and nonmagnetic Fe-Si silicide interface layers, while the nominal Si spacers turn out to be Fe-Si compound layers with additional amorphous Si sublayers only under the condition either $t_{\mathrm{Si}} \geq 3$ nm for the series $[\mathrm{Fe}(3\ \mathrm{nm})/\mathrm{Si}(t_{\mathrm{Si}})]_{30}$ or $t_{\mathrm{Fe}} < 2$ nm for the series $[\mathrm{Fe}(t_{\mathrm{Fe}})/\mathrm{Si}(1.9\ \mathrm{nm})]_{30}$ multilayers. A strong antiferromagnetic (AFM) coupling and negative magnetoresistance (MR) effect, about 1%, were observed only in multilayers with iron silicide spacers and disappeared when α-Si layers appear in the spacers. The dependences of MR on t_{Si} and on bilayer numbers N resemble the dependence of AFM coupling. The increase of MR ratio with increasing N is mainly attributed to the improvement of AFM coupling for multilayers with N. The t_{Fe} dependence of MR ratio is similar to that in metal/metal system with predominant bulk spin dependent scattering and is fitted by a phenomenological formula for GMR. At 77 K both the MR effect and saturation field H_{s} increase. All these facts suggest that the mechanisms of the AFM coupling and MR effect in sputtered Fe/Si multilayers are similar to those in metal/metal system.

PACS. 72.15.Gd Galvanomagnetic and other magnetotransport effects – 73.40.Sx Metal-semiconductor-metal structures

1 Introduction

The discovery of the giant magnetoresistance (GMR) effect related to the antiferromagnetic (AFM) interlayer exchange coupling in Fe/Cr multilayers [1] stimulated a great deal of research in various multilayers in the last ten years for understanding interesting physics and exploring useful properties. Fe/Si multilayers are a particular topic of research due to their potential technological applications in microelectronics and interesting antiferromagnetic interlayer coupling behavior [2–15]. Although a number of experimental work has been done to understand the mechanism of the interlayer coupling in this system, the results are controversial and it is not yet well understood how the formation of iron silicide in the spacer affects the coupling. The resistivity and magnetoresistance are sensitively dependent on the electronic structure of the multilayers, and thus their measurements can provide important information about electronic and magnetic properties of the multilayers. However, the studies of the transport properties on Fe/Si multilayers were very limited. Inomata *et al.* reported firstly their observation of a negative magnetoresistance (MR) effect with two different temperature dependences as a function of Si thickness and concluded that the magnetic coupling is mediated by a narrow gap semiconducting iron silicide for thin Si spacers [11]. However, recent research gave an opposite opinion that the AFM coupling in Fe/Si multilayers is attributed to the formation of metallic silicides in the interlayer [7,9,14,15]. In addition, the magnitude of the MR ratio found by Inomata *et al.* is very small (about 0.1% at room temperature) and whether the MR effect is associated with AFM coupling in Fe/Si multilayers is also questioned [12]. Moreover, the detailed data of the magnetic transport properties in Fe/Si multilayers, such as the dependencies of the resistivity and MR on the Fe and Si layer thicknesses and whole film thickness are not available in the literatures. In order to have a better understanding on the mechanism of the MR effect and the interlayer coupling in Fe/Si multilayers, more detailed study on transport properties in this system is needed. In this paper we present our study on the structure, magnetic and transport properties of sputtered Fe/Si multilayers with larger MR ratio of about 1% and $\Delta\rho \approx 2\ \mu\Omega$cm associated with AFM coupling. Our data suggest that the mechanism of the MR effect and

[a] e-mail: hrzhai@netra.nju.edu.cn

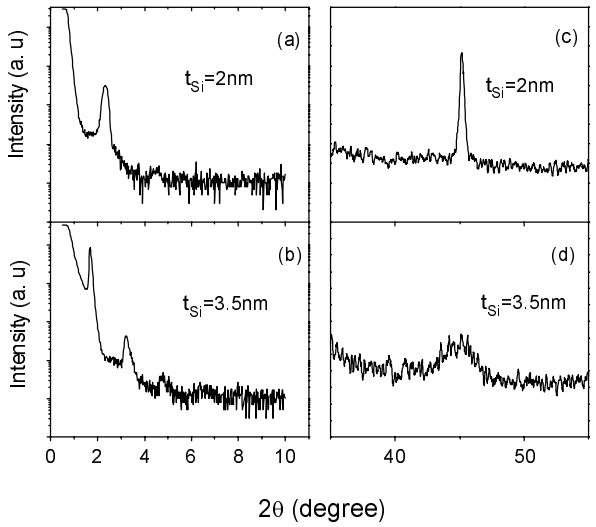

Fig. 1. Low-angle and high-angle X-ray diffraction patterns of $[\mathrm{Fe}(3\ \mathrm{nm})/\mathrm{Si}(t_{\mathrm{Si}})]_{30}$ multilayers with $t_{\mathrm{Si}} = 2$ nm, and 3.5 nm respectively.

interlayer coupling in sputtered Fe/Si multilayers is same as in metal/metal system.

2 Experimental

Several series of Fe/Si multilayers were deposited on water cooled glass and Si substrates by rf sputtering. The vacuum system had a base pressure of 5×10^{-7} Torr. An argon gas pressure of 5 mTorr was maintained during deposition. The layered structure was achieved by alternately exposing the substrate to Fe or Si targets *via* a rotating substrate holder controlled by a computer. The thicknesses of the sublayers were controlled by exposure time and deposition rate. To determine the deposition rate, several thick single layer films were first made and their thicknesses were measured by a talystep-type surface profilometer and by an optical interference method. The deposition rates of Fe and Si were controlled to be 0.09 and 0.06 nm/s. respectively. All the samples were deposited in the same condition.

The structure was characterized by both low- and high-angle X-ray diffraction (XRD). The samples were cut into bars of 2 cm $\times$ 0.2 cm for resistance and MR measurement by the standard four-probe method with an applied field in the film plane. The magnetic hysteresis loops were measured using a vibrating sample magnetometer (VSM) with a magnetic field of 0-20 kOe applied in the film plane. The signal due to the multilayers is obtained by subtracting the signal due to the substrate.

3 Results and discussion

3.1 Dependence on Si thickness

The first series of $[\mathrm{Fe}(3\ \mathrm{nm})/\mathrm{Si}(t_{\mathrm{Si}})]_{30}$ films were prepared with nominal Si layer thickness $t_{\mathrm{Si}} = 0.5{-}4.0$ nm, for exploring the Si layer thickness dependence of the magnetic and transport properties. Figure 1 shows two typical low- and high-angle X-ray diffraction (XRD) patterns of $[\mathrm{Fe}(3\ \mathrm{nm})/\mathrm{Si}(t_{\mathrm{Si}})]_{30}$ films with nominal Si layer thickness $t_{\mathrm{Si}} = 2$ nm, and 3.5 nm respectively. The low-angle X-ray diffraction peak at an angle 2θ satisfies the following relation [7]:

$$n^2\lambda^2 = 4\Lambda^2 \sin^2\theta + 2\delta \qquad (1)$$

where λ is the X-ray wavelength, $\Lambda = t_{\mathrm{Fe}} + t_{\mathrm{Si}}$ is the multilayer bilayer period to be determined and δ is the index of refraction for X-rays. Using the spacing between peak positions to eliminate the unknown δ from equation (1) gives the value of the bilayer period Λ. For the samples of $[\mathrm{Fe}(3\ \mathrm{nm})/\mathrm{Si}(2\ \mathrm{nm})]_{30}$ and $[\mathrm{Fe}(3\ \mathrm{nm})/\mathrm{Si}(3.5\ \mathrm{nm})]_{30}$, the derived modulation wavelengths Λ are 4.06 nm, and 5.6 nm, respectively, and are 0.94 nm and 0.90 nm shorter than the designed thicknesses, respectively. The reduction of the modulation wavelength indicates that there is a interdiffusion between Fe and Si layer. It is known that Fe-Si compounds are easily formed due to interdiffusion. Thus in this paper the layer materials, Fe and Si, and layer thicknesses are all nominal. In the high-angle XRD pattern ($2\theta = 20^\circ \sim 70^\circ$), only the Fe(011) diffraction peak appears. which is greatly broadened when $t_{\mathrm{Si}} \geq 3$ nm. The crystalline coherence length (ξ) of the films is obtained from the full width at half maximum (fwhm) by Scherrer formula [16]. For films with $t_{\mathrm{Si}} < 3$ nm, the coherence length is $\xi = 25$ nm, which is about four to five times of the bilayer period of the film, indicating a crystalline spacer with fairly good quality. For the films with $t_{\mathrm{Si}} \geq 3$ nm, the obtained coherence length is $\xi = 3.2$ nm, shorter than one bilayer period of the film, which, we assume, is due to the appearance of amorphous Si layer in the spacer [3]. It is noted that the coherence length ($\xi = 25$ nm) of our films for $t_{\mathrm{Si}} < 3$ nm is longer than those of Fullerton's sample ($\xi = 15$ nm) [3], implying that our samples have a better quality of crystalline structure.

The in-plane magnetic hysteresis loop measurements show an enhanced saturation field and reduced remanence in a broad range with the extreme around $t_{\mathrm{Si}} = 1.9$ nm, indicating AFM coupling, but no evidence of additional AFM coupling peaks for $t_{\mathrm{Si}} > 3$ nm. Figure 2a shows t_{Si} dependences of saturation field and remanence ratio for films of $[\mathrm{Fe}(3\ \mathrm{nm})/\mathrm{Si}(t_{\mathrm{Si}})]_{30}$, where t_{Si}= 0.5 to 4 nm. The AFM coupling is also identified by measurements of isotropic negative MR effect. Figure 2b shows the t_{Si} dependence of MR ratio for the films of $[\mathrm{Fe}(3\ \mathrm{nm})/\mathrm{Si}(t_{\mathrm{Si}})]_{30}$, t_{Si}= 0.5 to 4 nm. The peak position of MR ratio is nearly the same as that of the saturation field H_s and the minimum of remanence ratio. So, the MR effect found here is identified as being associated with the AFM coupling as in the metal/metal multilayers. Figure 3 shows typical M-H loops and MR-H cures for the sample of $[\mathrm{Fe}(6\ \mathrm{nm})/\mathrm{Si}(1.9\ \mathrm{nm})]_{30}$ multilayer at room temperature (RT) and 77 K, respectively. The MR ratio is 0.46% at room temperature (RT), and 0.74% at 77 K. It is shown that the saturation field H_s determined from in-plane M-H curves is nearly the same as that determined from MR-H curves, and both the MR ratio $\Delta\rho/\rho$ or MR $\Delta\rho$ and

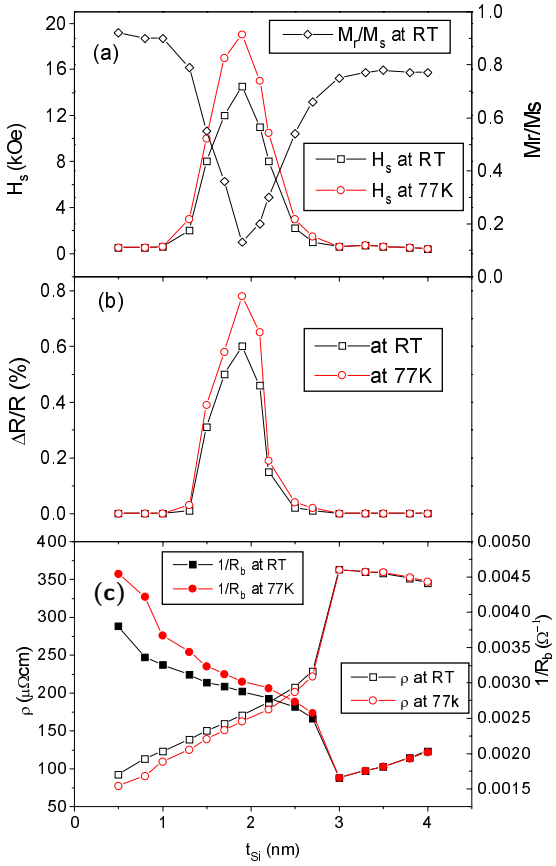

Fig. 2. The dependences of Si thickness on (a) saturation field and in-plane remanence ratio, (b) MR ratio at *RT* and 77 K, (c) resistivity ρ in zero field and $1/R_b$ at *RT* and 77 K for the films of $[\mathrm{Fe}(3\ \mathrm{nm})/\mathrm{Si}(t_{\mathrm{Si}})]_{30}$ with $t_{\mathrm{Si}} = 0.5$ to 4 nm.

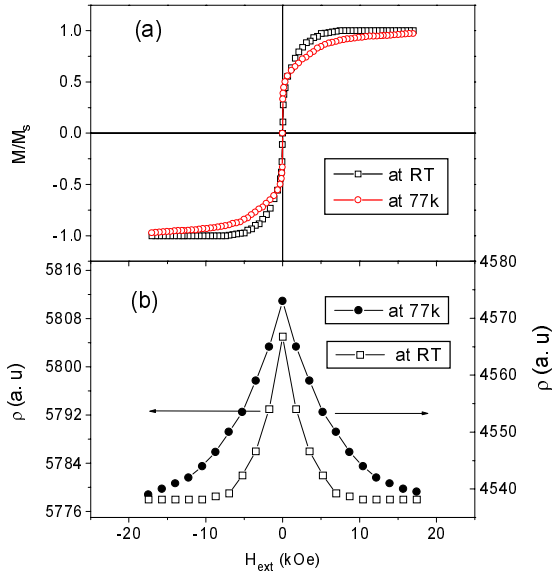

Fig. 3. The applied magnetic field dependences of magnetization and magnetoresistance for the sample of [Fe(6 nm) /Si(1.9 nm)]$_{30}$ multilayer. (a) In-plane M-H loops at *RT* and 77 K, (b) MR-H cure at *RT* and 77 K, respectively.

saturation field H_s increase at 77 K, while the resistivity ρ decreases with decreasing temperature. The increase of the interlayer coupling and MR and the decrease of the resistivity on cooling is a common nature in metal/metal system. An increase of the in-plane remanence ratio at 77 K was observed, consistent with previous observation on this system, which may be attributed to the increase of biquadratic coupling on cooling as shown by Fullerton [10]. Our results of the increase of both the saturation field and MR $\Delta\rho$ on cooling is incompatible with the speculation that the magnetic coupling across the Fe-Si spacers is mediated by the thermal excitation of charge carriers in the semiconducting spacers as suggested by several authors for their samples [4,11].

Figure 2c shows the variation of the resistivity ρ in zero field *versus* nominal Si layer thickness t_{Si} at *RT* and 77 K. It is shown that the resistivity increases with increasing t_{Si} for the films with $t_{\mathrm{Si}} < 3$ nm. Near $t_{\mathrm{Si}} = 3$ nm the resistivity increases rapidly, and when $t_{\mathrm{Si}} > 3$ nm it is nearly constant with a slight decrease tendency. The t_{Si} dependence of the resistivity in this system is quite peculiar and different from many different metallic multilayered system [23]. It can also be seen that with increasing t_{Si} the temperature dependence of the resistance is weakened and the sign of the temperature coefficient of the resistivity (TCR) changes for $t_{\mathrm{Si}} > 3$ nm films. It is known that Fe-Si silicide is easily formed at the interface due to atomic intermixing and interdiffusion, and the resistivity of Fe-Si silicide is much higher than the resistivity of Fe and has a weak temperature dependence [17]. Thus the peculiar t_{Si} dependence of the resistivity for $t_{\mathrm{Si}} < 3$ nm can be explained as mainly due to the increase of interdiffusion and the silicide formation with increasing t_{Si}. The rapid increase of the resistivity and changes of XRD data and the sign of TCR at $t_{\mathrm{Si}} \approx 3$ nm can be understood by that in addition to the Fe-Si layer an α-Si layer appears in the spacer for $t_{\mathrm{Si}} \geq 3$ nm. The appearance of α-Si layer in the spacers stops the increase of interdiffusion and results in the change of the slope in the figure in one hand, and prevents the AFM coupling in other hand.

To better understand the behavior of the resistivity ρ *versus* t_{Si} it is helpful to study the sheet resistivity of an individual Si (or Fe) layer in the multilayer stacks. If the multilayer is treated as a system of parallel conductors, the bilayer resistance per unit area R_b can be calculated [18]. R_b is equal to NR_T, where N is the number of bilayers of the multilayer and R_T, the total film resistance per unit area, is equal to ρ divided by the film thickness. From the data of $\rho \sim t_{\mathrm{Si}}$, $1/R_b\,(=(t_{\mathrm{Si}}+t_{\mathrm{Fe}})/\rho)$ is plotted *versus* nominal Si layer thickness (t_{Si}) as shown Figure 2c. It is seen that the dependence of $1/R_b$ *versus* nominal Si layer thickness t_{Si} for coupled films ($t_{\mathrm{si}} < 3$ nm) is quite different from that of the uncoupled films ($t_{\mathrm{Si}} > 3$ nm) due to different properties of spacer. For the coupled films ($t_{\mathrm{Si}} <$ 3 nm), as mentioned above, the α-Si layer is not formed in the spacer, therefore, the bilayer consists of Fe layer and Fe-Si silicide layer, and $1/R_b = 1/R_{\mathrm{Fe}} + 1/R_{\mathrm{Fe-Si}}$, where R_{Fe} and $R_{\mathrm{Fe-Si}}$ are the resistance values of Fe and Fe-Si layers within a bilayer, respectively. The values of R_{Fe}

and $R_{\mathrm{Fe-Si}}$ vary with t_{Si} due to increase of interdiffusion, which leads to a decrease of $1/R_b\,(=1/R_{\mathrm{Fe}}+1/R_{\mathrm{Fe-Si}})$ with increasing t_{Si}. When $t_{\mathrm{Si}} > 3$ nm, in addition to the Fe-Si layer the α-Si layer is formed in the spacer, and the bilayers consist of Fe, α-Si, and Fe-Si silicide interface layers. Also, $1/R_b = 1/R_{\mathrm{Fe}} + 1/R_{\mathrm{Si}} + 1/R_{\mathrm{Fe-Si}}$, where R_{Fe} R_{Si} and $R_{\mathrm{Fe-Si}}$ are the resistances of the Fe, α-Si and Fe-Si silicide interface layers, respectively. The resistance R_x is equal to ρ_x/t_x (resistivity / thickness), where x refers to Fe, α-Si and Fe-Si silicide. For $t_{\mathrm{Si}} > 3$ nm the resistances of R_{Fe} and $R_{\mathrm{Fe-Si}}$ are nearly constant. The inverse of the slope of the linear part (3 nm $< t_{\mathrm{Si}} <$ 4 nm) of the curve of $1/R_b$ *versus* t_{Si} gives the resistivity of α-Si layer in a bilayer as about $\rho_{\mathrm{Si}} \approx 280\ \mu\Omega$cm which is near the resistivity of a heavy impurity silicon. The impurity, which may reduce the resistivity of α-Si layer, may be present in our sputtered thin films. In the same way we will study below the intrinsic resistivity of Fe layers in the multilayers.

3.2 Dependence on Fe thickness

The second series of $[\mathrm{Fe}(t_{\mathrm{Fe}})/\mathrm{Si}(1.9\ \mathrm{nm})]_{30}$ multilayers was prepared with $t_{\mathrm{Fe}} = 0.5$ to 14 nm and $t_{\mathrm{Si}} = 1.9$ nm corresponding to the maximum AFM coupling. The magnetization of the film M_s defined as the measured magnetic moment divided by the volume of nominal Fe layer thickness t_{Fe} is determined from the in-plane magnetization curve measured by VSM. The relationship between $M_s t_{\mathrm{Fe}}$ and t_{Fe} is shown in Figure 4a, which can be described by a straight line $M_s(t_{\mathrm{Fe}}) = M_0(1 - 2d_0/t_{\mathrm{Fe}})$ [19,20], where M_0 is the average magnetization of Fe layers, d_0 refers to an effective dead layer thickness at each Fe/Si interface. By fitting the experimental data with a straight line as in Figure 4a, we obtain $M_0 = 1540$ emu/cm^3. This value of magnetization is smaller than the magnetization of 1730 emu/cm^3 for a single Fe film of 100 nm thick prepared by us in the same conditions, which is close to the bulk value of Fe. The low magnetization of the Fe layers M_0 in the multilayered structure is indicative of the diffusion of Si and also probably due to the lower density of the Fe in the layered structure as in other multilayered system [22]. From the interception of the fitted line with x axis in Figure 4a, the effective dead layer thickness is obtained as about $d_0 = 0.45$ nm. The zero magnetization moment of the dead layer at each Fe/Si interface may be ascribed to the heavy intermixing between Fe and Si, leading to the formation of a thin nonmagnetic Fe-Si interfacial layer.

It is interesting that when $t_{\mathrm{Fe}} < 2$ nm the Fe (110) diffraction peak in XRD pattern disappears, the sign of the temperature coefficient of the resistivity (TCR) also changes from positive to negative as shown in Figure 4c. In addition, the AFM coupling and negative MR were not observed though M_s still remains not zero for $t_{\mathrm{Fe}} > 0.9$ nm. These facts can be understood as the results of the change of the nominal Fe layer into mostly Fe-Si silicide interface layers and the appearance of α-Si layer in the spacer when nominal Fe thickness is made below 2 nm and Fe atoms are insufficient to diffuse into the Si spacer. The negative

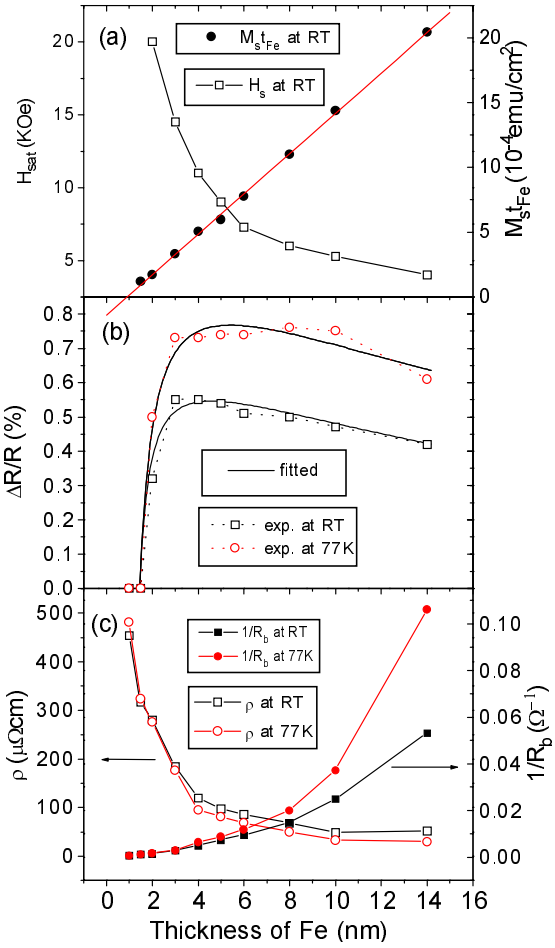

Fig. 4. The Fe layer thickness dependences of (a) saturation field H_s and M_s t_{Fe} at *RT*, (b) MR ratio at *RT* and 77 K, (c) resistivity in zero field and $1/R_b$ at *RT* and 77 K, respectively, for the films of $[\mathrm{Fe}(t_{\mathrm{Fe}})/\mathrm{Si}(1.9\ \mathrm{nm})]_{30}$ with $t_{\mathrm{Si}} = 1$ to 14 nm.

TCR for $t_{\mathrm{Fe}} < 2$ nm is a strong evidence of the appearance of α-Si in spacer, because the Fe-Si silicide has a very weak temperature dependence [17]. The formation of a ferromagnetic silicide layer and the dead layers at the interface of Fe is also consistent with the previous experimental results determined by spin- and angle-resolved photoemission method by Klässges *et al.* [15].

The saturation field H_s is inversely proportional to t_{Fe} for $t_{\mathrm{Fe}} \geq 2$ nm as shown in Figure 4a. The dependence of MR ratio on t_{Fe} is plotted in Figure 4b. The shape of MR *versus* t_{Fe} is different from that observed in Fe/Cr multilayers, for which MR ratio decreases monotonically with t_{Fe} for Fe layer thickness above 1 nm [21], demonstrating the dominant role of interfacial spin-dependent scattering in Fe/Cr. Here the broad maximum of MR at $t_{\mathrm{Fe}} \sim 5$ nm suggests that bulk spin-dependent scattering prevails in Fe/Si multilayers as found in some magnetic/nonmagnetic metallic system [23]. The Fe layer thickness dependence of the MR at *RT* and 77 K plotted in Figure 4b can be

well fitted by the following phenomenological formula for GMR [22,23]:

$$MR(t_{\mathrm{Fe}}) = \left(\frac{\Delta R}{R}\right)_0 \frac{1-\exp\left(-\frac{t_{\mathrm{Fe}}}{\lambda_\downarrow}\right)}{1+\frac{t_{\mathrm{Fe}}}{t_0}}. \qquad (2)$$

In this expression, the numerator is related to the probability for the scatter of spin-down electron as it traverses a ferromagnetic layer, while the denominator is related to the shunting effect of the current in the ferromagnetic layer. The normalization constant $(\Delta R/R)_0$ depends on the coupling between the ferromagnetic and nonmagnetic layers and on the thickness of the nonmagnetic spacers as well as on the number of periods. The fitted parameters of $(\Delta R/R)_0$ are about 22% at 77 K and 18.5% at *RT*, respectively. The larger value of $(\Delta R/R)_0$ at 77 K than that at *RT* is consistent with the behavior of MR. The parameters of t_0 corresponding to the shunting effect in ferromagnetic layer derived from the fit is 0.7 nm at 77 K, and 0.5 nm at *RT*, respectively. The value of $\lambda_\downarrow$ deduced from the fit as $\lambda_\downarrow = 15$ nm at 77 K and $\lambda_\downarrow = 13$ nm at *RT* gives an estimate of the mean free path (MFP) of the spin-down electrons in the Fe layers, which is larger than the modulation wavelengths, but smaller than the crystalline coherence length ($\xi = 25$ nm). The long electronic MFP is an important condition to observe MR effect in multilayers and it is related to the crystalline structure and coherence length. The coherence length of our coupled films ($\xi = 25$ nm) longer than that of previous samples is probably a major reason of longer $\lambda_\downarrow$ and larger MR effect in our Fe/Si multilayers.

Figure 4c shows the t_{Fe} dependence of the resistivity ρ of the multilayers at *RT* and 77 K. An overall decrease of the ρ with increasing t_{Fe} is contrary to the t_{Si} dependence of ρ shown in Figure 2c. It is shown that with increasing t_{Fe} the resistivity ρ decreases more slowly for $t_{\mathrm{Fe}} \geq 4$ nm than that for $t_{\mathrm{Fe}} < 4$ nm. The temperature coefficient of resistance (TCR), defined as TCR $= [\rho(297\ \mathrm{K}) - \rho(77\ \mathrm{K})]/[220\rho(297\ \mathrm{K})]$, decreases with decreasing t_{Fe} and changes sign for $t_{\mathrm{Fe}} < 2$ nm which is another evidence of the appearance of α-Si mentioned above. It is noted that the difference of the resistance between $\rho(297\ \mathrm{K})$ and $\rho(77\ \mathrm{K})$ are nearly constant for $t_{\mathrm{Fe}} \geq 4$ nm as shown in Figure 4c. A slight decrease of the TCR with decreasing t_{Fe} for $t_{\mathrm{Fe}} \geq 4$ nm is caused mainly by the slight increase of $\rho(297)$ due to increase of interface scattering when the t_{Fe} become smaller. When $t_{\mathrm{Fe}} < 4$ nm, the incoherent scattering at interfaces becomes more pronounced and finally α-Si layers appear, resulting in a more rapid increase of the resistance with decreasing t_{Fe}. Furthermore, the appearance of α-Si with negative TCR results in an compensation effect and leads to further decrease of TCR and finally its sign changes. Figure 4c also shows the t_{Fe} dependence of $1/R_b$. The sheet resistivity of individual Fe layers in the multilayers as a function of the Fe layer thickness is also studied following the method used in above section from the data of the inverse of the slope at different ranges on the curve of $1/R_b \sim t_{\mathrm{Fe}}$ shown in Figure 4c. It is found that with decreasing Fe layer thickness the resistivity of individual Fe layer increases, and the temperature dependence on the resistivity is also weakened. In the range of $t_{\mathrm{Fe}} = 10$ to 14 nm, the Fe layer resistivity is obtained as $\rho_{\mathrm{Fe}} \approx 14\ \mu\Omega$cm at *RT* (comparable to the bulk value of $\rho_{\mathrm{Fe}} = 9.8\ \mu\Omega$cm at *RT* [24]) and $\rho_{\mathrm{Fe}} \approx 5.6\ \mu\Omega$cm at 77 K. When $t_{\mathrm{Fe}} = 3$ nm the Fe layer resistivity is about $\rho_{\mathrm{Fe}} \approx 35\ \mu\Omega$cm at *RT* and does not change much down to 77 K. The increase of the resistance of Fe layer with decreasing Fe layer thickness is the result of the increase of interfacial scattering [25].

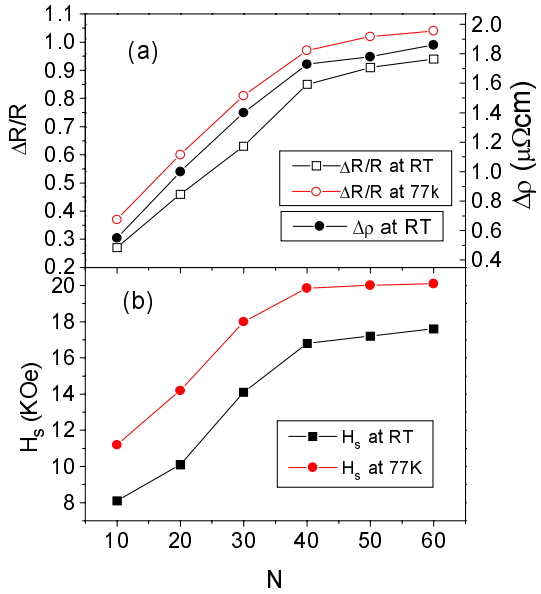

Fig. 5. The bilayer numbers N dependences of (a) MR ratio $\Delta\rho/\rho$ at *RT* and 77 K and MR $\Delta\rho$ at *RT*, (b) H_s at *RT* and 77 K, respectively, for the [Fe(3 nm)/Si(1.9 nm)]$_{\mathrm{N}}$ multilayers with $N = 10$ to 60.

3.3 Dependence on the number of bilayers

The third series is $[\mathrm{Fe}(3\ \mathrm{nm})/\mathrm{Si}(1.9\ \mathrm{nm})]_N$ multilayers with N varying from 10 to 60. It is shown in Figure 5 that the MR ratio $\Delta\rho/\rho$ increases with increasing N and approaches to a saturation values above $N = 40$. The saturation values are of 0.94% at room temperature and 1.05% at 77 K, which are largest values in our observations and in the literatures for sputtered Fe/Si multilayers. This kind of N dependence of the MR ratio $\Delta\rho/\rho$ is similar to that for many different magnetic multilayered systems [26]. It is well known that several factors may affect the dependence of MR on N [21]. Firstly, the two magnetic layers at either end of the multilayer contribute to MR by only half as much as the magnetic layers within the interior of the multilayer. This factor may be one of the origin of the dependence of MR on N. Secondly, when the whole film thickness is small compared to the mean free path in the multilayer, the MR increases with N because the electrons may propagate across many sublayers within a conduction carrier mean free path. However, for our samples the effective mean free path of 13 nm at *RT*

evaluated above is smaller than the thickness of our films (the smallest thickness is 40 nm for $N = 10$). So, the second argument may not be the main origin of the increase of MR ratio $\Delta\rho/\rho$ with increasing N and an additional origin may exist. It is found that the increase of MR ratio $\Delta\rho/\rho$ with increasing N in our samples is not due to the decrease of ρ but the increase of $\Delta\rho$ as shown in Figure 5a. In addition we observed that H_s also increases with N in the similar dependence as shown in Figure 5b. It is well known that $\Delta\rho/\rho$ and $\Delta\rho$ are affected by the degree of antiparallelism of the M_s in adjacent magnetic layers in demagnetized state and thus by the strength of AFM coupling. In other words, the increase of $\Delta\rho/\rho$ and $\Delta\rho$ with N may be related to the increase of coupling strength as found in previous work [3,7,13] in this system.

4 Conclusion

To sum up the above results and discussions we may draw the following main conclusions:

(1) The X-ray diffraction data, resistance and magnetic measurements demonstrate that in addition to the iron silicide at Fe/Si interface an α-Si layer begins to appear in the spacer when $t_{\mathrm{Si}} \geq 3$ nm for the first series of $[\mathrm{Fe}(3\ \mathrm{nm})/\mathrm{Si}(t_{\mathrm{Si}})]_{30}$ multilayers and $t_{\mathrm{Fe}} < 2$ nm for the second series of $[\mathrm{Fe}(t_{\mathrm{Fe}})/\mathrm{Si}(1.9\ \mathrm{nm})]_{30}$ multilayers. The nominal Fe layer generally consists of Fe layer, ferromagnetically ordered Fe-Si silicide layer, and nonmagnetic iron silicide dead layers at the interface of about 0.9 nm thickness.

(2) AFM coupling and negative MR effect were observed only in multilayers with iron silicide spacer. Both MR effect and AFM coupling disappear when α-Si layer appears in the spacer. The dependencies of MR ratio on t_{Si} and N resemble that of AFM coupling. An additional origin of the increase of MR ratio with increasing N is the improvement of AFM coupling in multilayers with larger N. The t_{Fe} dependence of MR ratio is similar to that in metal/metal system with predominant bulk spin dependent scattering and is fitted by a phenomenological formula for GMR. At 77 K both the MR effect and saturation field H_s increase. All these facts suggest that the mechanisms of the MR effect and AFM coupling in Fe/Si multilayers are similar to those found in ferromagnet / metallic spacer / ferromagnet system. The temperature dependence of the MR for our samples is different from the observation by Inomata *et al.* [11] in which the AFM coupling is considered to be originated from a narrow gap semiconducting Fe-Si spacer for their samples, in contrast to our samples in which the AFM coupling and MR effect are induced by metallic Fe-Si spacer.

(3) The maximum value of MR ratio, $\Delta\rho/\rho \sim 1\%$, found here is largest value of sputtered Fe/Si multilayers reported in the literatures. Though the MR ratio is still much smaller than that of Fe/Cr or Co/Cu multilayers, but the maximum value of $\Delta\rho$ is about 2 $\mu\Omega$cm which is comparable to that of Fe/Cr multilayers ($\Delta\rho =$ 3 $\mu\Omega$cm [27]). The larger MR value seems to be related to the longer coherence length and MFP in our sputtered samples.

This work is supported by National Natural Science Foundation of China, Chinese State Education Commission.

References

1. M.N. Baibich, J.M. Broto, A. Fert, F. Nguyen Van Dau, F. Petroff, P. Etienne, G. Creuzet, A. Friederich, J. Charelas, Phys. Rev. Lett **61** 2472 (1988).
2. S. Toscano, *et al.*, J. Magn. Magn. Mater. **114**, L6 (1992).
3. E.E. Fullerton, *et al.*, J. Magn. Magn. Mater. **117**, L301 (1992).
4. J.E. Mattson, *et al.*, Phys. Rev. Lett. **71**, 185 (1993).
5. B. Briner, M. Landolt, Phys. Rev. Lett. **73**, 340 (1994).
6. K. Inomata, S.N. Okuno, Y. Saito, K. Yusu, J. Magn. Magn. Mater. **156**, 219 (1996).
7. A. Chaiken, R.P. Michel, M.A. Wall, Phys. Rev. B **53**, 5518 (1996).
8. J.A. Carlisle, *et al.*, Phys. Rev. B **53**, R8824 (1996).
9. J. Kohlhepp, F.J.A. den Broeder, J. Magn. Magn. Mater. **156**, 261 (1996).
10. E.E. Fullerton, S.D. Bader, Phys. Rev. B **53**, 5112 (1996).
11. K. Inomata, K. Yusu, Y. Saito, Phys. Rev. Lett. **74**, 1863 (1995).
12. F.J.A. den Broeder, J. Kohlhepp, Phys. Rev. Lett. **75**, 3026 (1995).
13. J. Kohlhepp, F.J.A. den Broeder, M. Valkier, A. Van der Graaf, J. Magn. Magn. Mater. **165**, 431(1997).
14. J.A. Carlisle, A. Chaiken, R.P. Michel, L.J. Terminello, J.J. Jia, T.A. Callcotl, D.L. Ederer, Phys. Rev. B **53**, R8824 (1996).
15. R. Klasges, C. Carbone, W. Eberhardt, C. Pampuch, O. Rader, T. Kachel, W. Gudat, Phys. Rev. B **56**, 10801 (1997).
16. D.B. Cllity, *Elements of X-Ray Diffraction* (edited by Addison-Wesley, 1978, London).
17. G. Marchal, Ph. Mangin, Ch. Janot, Solid State Commun. **18**, 739 (1976).
18. J.D. Jarratt, T.J. Klemmer, J.A. Barnard, J. Appl. Phys. **81**, 5793 (1997).
19. R.V. Leauwen, C.D. England, J.R. Dutcher, C.M. Falco, W.R. Bennett, B.Hillebrands, J. Appl. Phys. **67**, 4910 (1990).
20. J.R. Childress, C.L. Chier, A.F. Jankowski, Phys. Rev. B **45**, 2855 (1992).
21. S.S.P. Parkin, E-MRS spring meeting, strasbourg, Mag 90, Paper c-//-2.
22. C. Cowache, *et al.*, Phys. Rev. B **53**, 15027 (1996).
23. B. Dieny, *et al.*, Phys. Rev. B **45**, 806 (1992).
24. T.R. Mcguire, R.I. Potter, IEEE Trans. Mag. **MAG-11**, 1018 (1975).
25. K.L. Chopra, *Thin Film Phenomena* (McGraw-Hill, New York, 1969), p. 345.
26. B. Dieny, J. Phys. Cond. Matter **4**, 8009 (1992).
27. J.M. Colino, I.K. Schuller, V. Korenirski, K.V. Rao, Phys. Rev. B **54**, 13030 (1996).